Advances in Thermal Processes
and Energy Transformation
Volume 2, 2019, Bely02, p. 19-23
ISSN 2585-9102

Performance of the Adsorptive Solar Refrigerators Based on Composite Adsobents 'Silica Gel – Sodium Sulphate'

Elena A. Belyanovskaya[1] ● Grigoriy N. Pustovoy[1] ● Yana O. Sergiyenko[2]● Kostyntyn M. Sukhyy[2] ● Oleksandr O. Yeromin[3] ● Elena M. Prokopenko[3] ● Mikhailo V. Gubinskyi[4]● Ján Kizek[5]

[1]Department of Power Engineering, State Higher Education Institution 'Ukrainian State University of Chemical Engineering', Gagarine av. 8, Dnipro, Ukraine, belyanovskaya@voliacable.com
[2]Department of Polymer and Nanocomposites, State Higher Education Institution 'Ukrainian State University of Chemical Engineering', Gagarine av. 8, Dnipro, Ukraine
[3]Department of Ecology, Heat Transfer and Labour Protection, National Metallurgical Academy of Ukraine, Gagarine av. 4, Dnipro, Ukraine
[4]Department of industrial power system, National Metallurgical Academy of Ukraine, Gagarine av. 4, Dnipro, Ukraine
[5]Technical university of Košice, Faculty of Materials, Metallurgy and Recycling, Institute of Metallurgy, Letná 9, 042 00 Košice, Slovak Republic

Category : Original Scientific Paper
Received : 21 March 2019 / Revised: 29 March 2019 / Accepted: 30 March 2019

Keywords : adsorptive refrigerator, net coefficient of performance, adsorptive capacity, composite adsorbent.

Abstract : The performance of adsorptive solar refrigerators based on composite adsorbents 'silica gel - sodium sulphate' is studied. An optimum composition of adsorbent 'silica gel – sodium sulphate' is suggested to be of 20 % silica gel and 80 % sodium sulphate. The basic factors affected the net coefficient of energy performance of the adsorptive solar refrigerator were stated. Net coefficients of performance of solar adsorptive refrigerator based on composite 'silica gel – sodium sulphate' are stated to change from 0.25 to 0.34 during operating period. Utilization of the adsorption heat is suggested to warm the heat carrier which applied to heat adsorbent during regeneration.

Citation: Belyanovskaya, Elena A., et al.: Performance of the Adsorptive Solar Refrigerators Based on Composite Adsobents 'Silica Gel – Sodium Sulphate', Advance in Thermal Processes and Energy Transformation, Volume 2, Nr. 1, (2019), p. 19-23, ISSN 2585-9102

1 Introduction

Simultaneous growth of prices of fossil fuels and energy carriers rates requires alternative to traditionally used steam compression refrigeration devices which supply a significant amount of electricity, and complicate the utilization of thermal energy.

A promising alternative to such systems is adsorption refrigeration solar devices, the so-called solar adsorption refrigerators, which allow to use of unconventional sources of low-potential thermal energy and environmentally friendly chilling agents.

As a rule, adsorption refrigeration solar systems include a solar collector, an adsorber, a condenser and an evaporator located near the refrigerating chamber. Their operation is usually performed in two stages. The first is the adsorption and evaporation of the refrigerant, due to which the temperature in the refrigerating chamber decreases, the second being the regeneration of the adsorbent, that is, the desorption and condensation of the chilling agent. During the second stage, the adsorbent is heated to the regeneration temperature by external sources. Ammonia [1], water [2], ethanol [1] and methanol [1] are used as chilling agents. Most of them are environmentally dangerous, but also water being available. Activated carbon [1] silica gel [2], zeolite [1], salts of $MnCl_2$, NH_4Cl, strontium chloride, sodium bromide [3] are used as adsorbents. Typical adsorbents, in particular, zeolites and silica gels, have a high regeneration temperature more than 100°C and a low adsorptive capacity, which not only involves the use of large quantities of adsorbent, but also strongly limits the potential of the heat source.

A higher adsorption capacity is stated for massive salts. However, the exploitation of massive salts is complicated by their corrosive activity. Furthermore, the hydration of massive salts in the stationary mode results in the formation of hydrated films that block the access of moisture to anhydrous salts, which significantly slows down the process of adsorption and cooling. As a consequence, the cycling of massive salts is impossible without mechanical dispersion during operation.

The way to solve this problem is creating composite adsorbents 'salt in a porous matrix'. Examples of such materials are adsorbents $CaCl_2$ / expanded graphite [4], $BaCl_2$/ vermiculite [5], LiCl / silica gel [6], as well as nanodispersed composite adsorbents synthesized by the sol – gel method, namely, sodium sulphate /silica gel [7, 8].

Obviously, adsorbent properties strongly affect the coefficient of energy performance. Nevertheless, despite the various types of adsorbents a significant amount of adsorption heat is wasted when adsorptive refrigerator operated.

In this regard, the aim of present work is to suggest methods for storage of adsorption heat and to study the correlation of the performance characteristics of solar adsorptive refrigeration devices and the properties of the composites 'silica gel-sodium sulphate' synthesized by the sol-gel method.

2 Experimental

The main structural elements of the adsorption refrigerator [9], according to Fig. 1, are the adsorber (1), the condenser (7) and the evaporator (4) located in the cold box (6).

A transparent SAN polycarbonate plastic (8 mm thick) with an integral transmittance of 0.88 is installed on the front side of the adsorber, and the composite adsorbent 'silica gel-sodium sulphate', which was synthesized according to [7], is located in the lower part. Water is used as a refrigerating fluid. The 2.29 m^3 refrigerator compartment is made of steel grade 30X 0.5 mm thick. Polystyrene foam was used as thermal insulation.

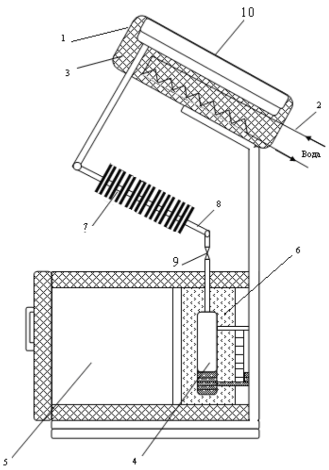

Figure 1 Adsorption refrigerator:
1 - adsorber; 2 – coil pipe; 3 - adsorbent; 4 - evaporator; 5 – cold box; 6 – cold storage unit; 7 - condenser; 8 - pipe; 9 - tap [9].

Chilling proceeds due to evaporation of water and adsorption, and regeneration of the adsorbent, followed by desorption and condensation of water. The operation is carried out in two stages. The first stage is getting cold. When the tap (9) opened, water vapour begins to diffuse through the condenser to the adsorber. Due to the adsorption of water by the adsorption material it evaporates in the evaporator (4), creates a cooling effect in the cold box (5). Since a large volume of water is contained in the walls of the refrigerator, the cold in the chamber (5) is maintained at 5–10°C for 10–20 hours until the next cycle. When water is sorbed by the adsorbent (3), the temperature in the adsorber (1) increases significantly due to the release of heat of adsorption. It can be used for heating the water in the coil pipe which can be used to warm the adsorbent during the second stage.

The second stage is the regeneration of the adsorbent. As the tap 9 closed, the adsorbent (3) is heated by solar energy. The water is collected in the condenser (7) and then drained into the evaporator (4) and the process of getting cold begins.

The amount of heat that is required to be taken from the cold box during the day was calculated according to [10] as the sum of the heat going to cool the chamber itself and the introduced food substances and to cover the heat inleaks both of the chamber and when opening the chamber when adding products:

$$Q_1 = C \cdot m \cdot \Delta T + C_{pr} \cdot m_{pr} \cdot \Delta T + \sum Q_z \qquad (1)$$

C is the heat capacity of the structural elements, $kJ.kg^{-1}.K^{-1}$; C_{pr} is the heat capacity of the food substances introduced into the refrigerating chamber, $kJ.kg^{-1}.K^{-1}$; ΔT is the difference between ambient temperature and average daily temperature in the refrigerating chamber, K; m, m_{pr} is mass of the cold box and introduced products, respectively, kg; ΣQ_z is the sum of heat leakage into the chamber as a result of heat transfer through its walls, floor and ceiling, from infiltration of outside air when the chamber is opened and loads from lighting, kJ.

Heat inleak into the cold box by heat transfer during the day was determined according to [11] as the product of heat load during heat transfer through the walls, floor and ceiling of the chamber and the period of operation:

$$Q_{ht} = K \cdot F \cdot \Delta t \cdot \tau \quad (2)$$

where Q_{ht} is heat inleaks because of heat transfer, kJ; K is the heat transfer coefficient of $kW.m^{-2}.K^{-1}$; F is the area of the outer surface of the chamber, m^2; τ is the period of operation during the day, s; Δt is the temperature difference between the air on both sides of the wall, °C.

Heat transfer coefficient was calculated according to [11]:

$$K = \frac{1}{\left(\frac{1}{\alpha_{v1}} + \frac{\delta}{\lambda_m} + \frac{\delta_{iz}}{\lambda_{iz}} + \frac{1}{\alpha_{v2}}\right)} \quad (3)$$

where α_{v1} and α_{v2} are heat transfer coefficients for air inside and outside the cold box, $kW.m^{-2}.K^{-1}$, respectively; δ and δ_{iz} are wall thickness of the refrigerating chamber and heat insulation, m; λ_m and λ_{iz} are the thermal conductivities of the walls of the refrigerating chamber and thermal insulation, $kW.m^{-1}$ K^{-1}.

Heat inleak into the cold box due to the opening of the doors Q_{inf} [11], was calculated as the product of the heat load and the duration of the opening of the doors during the day:

$$Q_{inf} = q \cdot D_{\tau} \cdot D_f \cdot (1 - E) \cdot \tau_{op} \quad (4)$$

where q is the total daily heat load on the cold box for the air flow, fully established taking into account the difference in density, heat and moisture content of indoor and outdoor air, as well as the size of the door opening, kW; D_τ is coefficient taking into account the time when the doors are open during the day; D_f is coefficient taking into account the nature of the air flow in the doorway; E is the degree of effectiveness of the doorway security device; τ_{op} is the time when the doors are open during the day, s.

Thermal inflows as a result of the work of lighting devices were defined as the product of the number of luminaires, luminaire power and the period of operation during the day [11].

The heat is taken from the cold box due to the evaporation of water in the evaporator. The amount of heat taken from the cold box when water evaporated can be calculated as:

$$Q_2 = \Delta H_{ev} \cdot m_w \quad (5)$$

where ΔH_{ev} is evaporation heat of water, kJ/kg; m_w is mass of water, kg.

From here the mass of water can be calculated to ensure the selection of the required amount of heat in the cold box.

To compensate for daily fluctuations in weather conditions, the mass of working fluid is proposed to increase by 50%. Thus, the mass of water in the evaporator will be 33.29 kg.

On the basis of the adsorption capacity of the silica gel / Na_2SO_4 composite, according to the data of [8], it is possible to calculate the mass of the adsorbent, which must be placed in the adsorber. The amount of heat required for the adsorbent regeneration (Q_3, kJ) can be calculated by the formula:

$$Q_3 = m_k \cdot C_k \cdot \Delta T_1 + m_w \cdot C_w \cdot \Delta T_1 + m_B \cdot \Delta H_{des} \quad (6)$$

where ΔT_1 is the difference between the temperature of the adsorbent and the temperature of regeneration, K;

ΔH_{des} is the heat of desorption of water, $kJ.\ kg^{-1}$;

m_k and m_w are respectively, the mass of the composite and the adsorbed water, kg;

C_k and C_w are the heat capacity of the composite and water, respectively, $kJ.kg^{-1}.K^{-1}$.

The net coefficient of performance was defined as the ratio of the amount that is taken in the refrigerating chamber when water evaporates, and the heat consumption for the regeneration of the adsorbent, that is:

$$\varepsilon_n = \frac{Q_1}{Q_s} \quad (7)$$

where ε_n is the net coefficient of performance; Q_1 is the amount of heat that must be removed from the refrigerating chamber, kJ; Q_s is the amount of solar energy which supply to system, kJ.

The value of Qs is corresponded to product of surface of solar collector and solar radiant flux.

So, the surface area of solar collector can be calculated according to [12]

$$F_k = \frac{Z_k \cdot Q_3}{Q_k} \quad (8)$$

where F_k is surface area of collector, m^2; Q_3 is the amount of heat required for the adsorbent regeneration, MJ; Q_k is the amount of heat which supplied by 1 m^2 of solar collector, $MJ.m^{-2}$; Z_k is the coverage factor which considered irregularity of solar radiation during a day or a season.

3 Results and discussion

Obviously, an increase in the content of sodium sulphate in the composite is stated to contribute to a decrease in the mass of the composite, and, consequently, the amount of heat that must be spent on the regeneration of the adsorbent. The minimal mass of adsorbent of 24.68 kg is stated for composites containing, wt. %: silica gel – 20 and sodium sulphate – 80.

The amount of heat for regeneration of the composite Q_3, and, consequently, the coefficient of performance, is significantly affected by the difference in the temperature of the adsorbent and the temperature of regeneration ΔT_1.

With it decreased, a monotonous growth in the coefficient of performance is observed. The maximum values of ε are established at ΔT_1 = 55 ° C.

Results of calculation of net coefficient of performance are given in the Table 1.

The maximal values of ε_n are observed in September which corresponded to minimal solar radiant flux. According to data M.S. Fernandes et al. [13] net coefficients of performance of chilling units based on pair ’silica gel – water’ does not exceed 0.2. For pair ’zeolite – water‘ these values are at most 0.3. So, the efficiency of solar adsorptive refrigerator based on ’silica gel – sodium sulphate’ conforms to the system with the same calling agent.

Due to exothermic character of water vapour adsorption, operating the adsorptive chiller is accompanied by evolution of a significant amount of heat. It is advisable to consider possibility of its utilization.

Traditional procedure can be using the adsorption heat to warm a heat carrier which applied to heat the adsorbent during regeneration.

Water mass and temperature after adsorption can be estimated by equations of heat balance. Results of calculations are presented in the Table 2.

Obviously, as temperature difference increased, water mass is decreased. At the temperature difference 65 – 75°C temperature of water after adsorption is 80 – 90°C, water mass being 277,8 – 332,1 kg (277,8 – 332,1 l).

Table 1 Net coefficients of performance of solar adsorptive refrigerator based on composite ‘silica gel – sodium sulphate’

Month	Daily solar radiant flux, MJ/m^2	Heat supplied by solar collector, MJ	Net coefficient of performance
May	21.56	214.56	0.25
June	21.09	209.90	0.26
July	21.81	217.06	0.25
August	20.37	202.74	0.27
September	15.87	157.96	0.34

Table 2 Results of calculation of water mass and temperature after adsorption

Δt, °C	M_{H2O}, kg	Temperature of water after adsorption, °C
35	681.4	50
45	513.2	60
55	406	70
65	332.1	80
75	277.8	90

So, obtained heat carrier can be used for warming the adsorbent in morning period.

4 Conclusion

The processes of operation of the solar adsorptive refrigerator based on composite adsorbents ’silica gel - sodium sulphate’ were studied. The main technological parameters affected the net coefficient of performance are revealed.

An increase in the value of the coefficient performance was established with a decrease in the temperature difference between the adsorbent and the regeneration temperature ΔT_1.

It is established that the maximum values of the refrigeration coefficient correspond to ΔT_1 = 55°C for composites that contain about, mass. %: silica gel – 20 and sodium sulphate – 80.

Utilization of the heat of adsorption is proposed to warm the heat carrier which applied to heat adsorbent during regeneration. The possibility of water heating due to the heat of adsorption from 50 to 90°C is shown, the water mass being 277 – 681 kg.

5 The reference list

[1] SANTORI, G., DI SANTIS, CH.: Optimal fluids for adsorptive cooling and heating, *Sustainable Materials and Technologies*, Vol. 12, pp. 52 – 61, 2017

[2] LU, Z.S., WANG, R.Z., XIA, Z.Z., WU, Q.B., SUN, Y.M., CHEN, Z.Y.: An analysis of the performance of a novel solar silica gel–water adsorption air conditioning, *Applied Thermal engineering*, Vol. 31, № 17 – 18, pp. 3636 – 3642, 2011.

[3] BAO, H.S., OLIVEIRA, R.G., WANG, R.Z., WANG, L.W., MA, Z.W.: Working pairs for resorption refrigerator, *Applied Thermal Engineering*, Vol. 31, № 14 – 15, pp. 3015 – 3021, 2011

[4] LI, S.L., XIA, Z.Z., WU, J.Y., LI, J., WANG, R.Z., WANG, L.W.: Experimental study of a novel $CaCl_2$/expanded graphite-NH_3 adsorption refrigerator, *International Journal of Refrigeration*, Vol. 33, № 1, 61 – 69, 2010.

[5] ZHONG, Y., CRITOPH, R.E., THORPE, R.N., TAMAINOT-TELTO, Z., ARISTOV, YU.I.: Isothermal sorption characteristics of the $BaCl_2$–NH_3 pair in a vermiculite host matrix, *Applied Thermal Engineering*, Vol. 27, № 14–15, pp. 2455 – 2462, 2007.
[6] MAGGIO, G., GORDEEVA, L.G., FRENI, A., ARISTOV, YU.I., SANTORI, G., POLONARA, F., RESTUCCIA, G.: Simulation of a solid sorption ice-maker based on the novel composite sorbent “lithium chloride in silica gel pores”, *Applied Thermal Engineering*, Vol. 29, № 8 – 9, pp. 1714 – 1720, 2009.
[7] SUKHYY, K., BELYANOVSKAYA, E., KOVALENKO, V., KOTOK, V., SUKHYY, M., KOLOMIYETS, E., GUBYNSKYI, M., YEROMIN, O., PROKOPENKO, O.: The study of properties of composite adsorptive materials “silica gel – crystalline hydrate” for heat storage devices, *Eastern-European Journal of Enterprise Technologies*, Vol. 91, № 1, pp. 52 – 58, 2018.
[8] SUKHYY, K. M., BELYANOVSKAYA, E. A., KOZLOV, YA. N., KOLOMIYETS, E. V., SUKHYY, M. P.: Structure and adsorption properties of the composites ‘silica gel – sodium sulphate’, obtained by sole gel method, *Applied Thermal Engineering*, Vol. 64, pp. 408 – 412, 2014.
[9] Pat. 86227 Ukraina, MPK F 25 B 17/00. Adsorptsiyniy kholodilnik / Sukhyy K.M., Sukhyy M.P., Kolomiyets O.V. [ta in.]; Dergavniy vischthiy navchalniy zaklad “Ukrainskiy dergavniy khimiko-tekhnologitcheskiy universitet”. – № u 2013 05136; zayavl. 22.04.2013 opubl. 25.12.2013, Bul. № 24 (in Ukrainian)
[10] KOLOMIYETS, O.V., BELYANOVSKA, O.A., SUKHYY, K.M., PROKOPENKO, O.M., KOZLOV, YA.M., SUKHYY, M.P.: Osnovni robochi kharakteristiki sonyachnogo adsorbtsiynogo kholodilnika na osnovi kompositnogo sorbentu «silikagel/Na_2SO_4, Odeska natsionalna akademiya kharchovyh tekhnologiy. Naukovi pratsi, Vol. 2, № 47, pp. 176 – 181, 2015 (in Ukraine)
[11] Rukovodstvo po raschetu teplovogo balansa kholodilnykh kamer i vyboru osnovnykh proektnykh parametrov kholodylnykh ustanovok, M.: Ostrov, 1999 (in Russian)
[12] SUKHYY, K.M., BELYANOVSKAYA, E.A., KOLOMIYETS E.V.: Design and performance of adsorptive transformers of heat energy. Riga, Latvia: LAP Lambert Academic Publishing, 2018.
[13] FERNANDES, M.S., BRITES, G.J.V.N. COSTA, J.J., GASPAR, A.R., COSTA, V.A.F.: Review and future trends of solar adsorption refrigeration systems, *Renew. Sustain. Energy Rev.* Vol. 39, pp. 102 – 123, 2014.

Acknowledgement
This article was supported within the framework of budget project 0119U002243.

Advances in Thermal Processes
and Energy Transformation
Volume 2, 2019, Flim02, p. 24-27
ISSN 2585-9102

Alternative Measurements of Heat Flow Density in Space

Marián Flimel[1]

[1]Department of Process Technique, Technical University of Košice, Faculty of Manufacturing Technologies with a seat in Prešov, Štúrova 31, 080 01 Prešov, e-mail: marian.flimel@tuke.sk

Category : Application
Received : 21 June 2019 / Revised: 28 June 2019 / Accepted: 29 June 2019

Keywords : heat flow density, measurement, space

Abstract : The article is focused to alternative measurement of heat flow density in space. There is describe the construction of this equipment. The device will be used to determine heat loss through walls in buildings, pipework, cold stores, heat storage systems (U value), further to calorimetry, measuring the thermal characteristics of substances and technical applications in which temperature difference is used as a control variable. The device allows measurements in situ conditions.

Citation: Flimel Marián: Alternative Measurements of Heat Flow Density in Space, Advance in Thermal Processes and Energy Transformation, Volume 2, No.2 (2019), pp. 24-27, ISSN 2585-9102

1 Introduction

Thermal comfort or thermal discomfort are two diametrically opposed conditions, which one feels in the internal environment of buildings. Boundary between the subjectively perceived states of perception of the human satisfaction with the environment should be verified by objective measurements. The purpose of this paper is to describe a measuring system for determining the density of heat flow in the environment.

Table 1 Interaction of person with thermal environment – their elements [1,2]

Thermal comfort = balance between person and environment should be ensured by:
- Indoor temperature
- Medium radiation temperature
- Air velocity
- Isolation of human clothing
- Resistance of clothing against the evaporation of sweat
- Human metabolism
- Occupation – activity
Thermal discomfort creates
- Heat radiation asymmetry
- Excessive temperature gradient of air
- Draught, air flow
- Too hot or cold floor
- Too hot or cold ceiling

Table 1 shows the thermal discomfort such as too cold or hot floor or ceiling. This may be also a cold window glass in winter or hot radiator or technology or excessive radiation through the same glass in solar radiation. What are these values in relation to legislative requirements? - It is necessary to determine it by measurements.

2 Heat transfer in the space and the reasons for the measurement of heat flows

In the interiors of buildings, the heat spreads by convection, conduction and radiation. Imagine a three-dimensional space of coordinates (x, y, z) and there a person in an activity. Climatic conditions of space are non-stationary by the influence of:

- non-stationary conditions in the exterior and adjacent interiors; a heat flow takes place between our three-dimensional space and surrounding through building structures,
- in the interior of the considered space, there can be made a fluctuation of climate conditions by machines̓ activity or other technology of environment (heating system, lighting, ventilation, air conditioning, etc.), thereby it also changes the heat flows in the interior.

Spread of heat flows in the space (in the air) may be varied. Heat flows have the following parameters [3]:

a) its size - value ($W.m^{-2}$),
b) direction (with respect to coordinates x, y, z),
c) spatial distribution,
d) exposure – contact time,
e) features: what is the nature of the heat flow – the heat flow by circulation (convection) Q_c or the heat flow by radiation Q_r.

The measurement of the total heat flow density by convection and radiation in situ may be performed by using heat plate to measure the heat flow density. Heat flow sensor was originally designed to measure the value U in building structures (walls).

3 Measuring principle, heat flux sensor plates (wall for measuring U value) [4]

Heat flux plates are sensitive sensors permitting precise measurement of heat flow densities (***q***) (= energy per time and surface). A heat flux sensor plate laid on the measuring point to be tested generates a resistance to the heat flow it thus restricts. As heat passes through the thickness of the plate a temperature gradient is formed proportional to the density of the heat flow.
Heat flux sensor plates comprise a meander array of numerous inversely connected thermocouples embedded in a substrate. With thick substrate materials the plates are designed with a margin round the meander array sufficient to prevent free lateral circulation of the heat flow. The heat flow values obtained always refer to the surface covered by the meander array; they are averaged over this surface. These active sensors provide signals in the millivolt range that can be evaluated fairly easily.

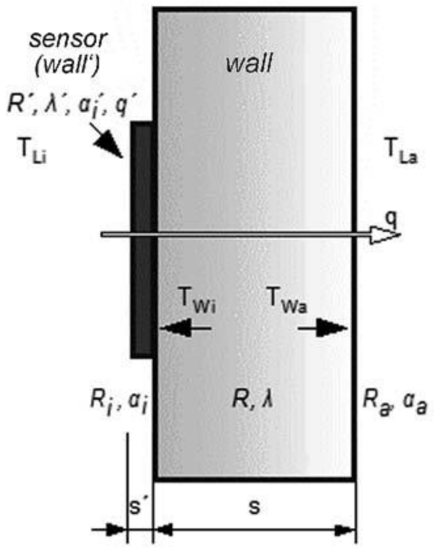

Figure 1 : Measuring principle U value [4]

T_{Li} = Air temperature, inside [°C]
T_{La} = Air temperature, outside [°C]
T_{Wi} = Wall temperature, inside surface [°C]
T_{Wa} = Wall temperature, outside surface [°C]
q = Heat flow density [$W.m^{-2}$],
R = Thermal conductance resistance of the wall layer(s) [$m^2K.W^{-1}$]
R_i = Thermal surface transfer resistance on the inside of the structural element [$m^2.K.W^{-1}$]
R_a = Thermal surface transfer resistance on the inside of the structural element [$m^2.K.W^{-1}$]
α_i = Thermal surface transfer coefficient, inside [$W.m^{-2}.K^{-1}$]
α_a = Thermal surface transfer coefficient, outside [$W.m^{-2}.K^{-1}$]
λ = Thermal conductivity of the wall layer(s) [$W.m^{-1}.K^{-1}$]
s = Thickness of the wall layer(s) [m]
U = Thermal transmittance coefficient [$W.m^{-2}.K^{-1}$],
$U = q : (T_{Li} - T_{La})$

<u>Alternative use of heat flux plates ALMEMO</u>

Heat flux plates are used in a wide variety of areas in the natural sciences and applied technology.
1. To determine heat loss through walls in buildings, pipework, cold stores, heat storage systems (U value).
2. Calorimetry, measuring the thermal characteristics of substances.
3. Technical applications in which temperature difference is used as a control variable.
4. Another suggested possibility according to Figure no. 2 is the determination of the heat flow density of q ($W.m^{-2}$) in workplace air, the heating and convection element at a certain distance from the surfaces, which radiate them.

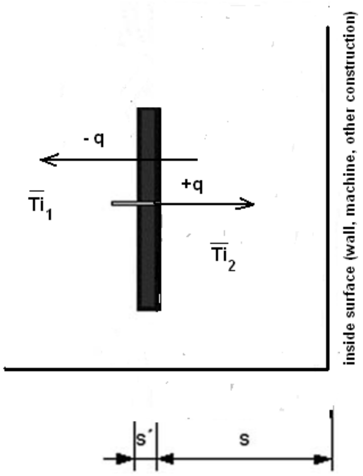

Figure 2 Measuring principle q value [5]

4 The sequence of development of system for the measurement of q- value

Plate is used for the system (type of the marked plate FQ A018C + ZA 9007-FS) to the measuring system ALMEMO 2290-8 of Ahlborn Company.

It is possible to construct the system for measuring the value in one direction in space (e.g. x direction), or in two or three directions of the considered point in space:

1. Prepare 1, 2 or three plates, according to the measuring need.
2. Construct a structure to attach the plates of heat insulting and heat resistant material for two or three plates. Fix the plates to the side frame so that the sufficient space remains between them for airflow (Figure 4). If only one plate is applied, only one hanging hitch is made on the stand (Figure 3).
3. Join together the cable line from the plates.
4. Integrate the connectors to the device Almemo 2290-8.
5. Take measurements (immediate or continuously recorded)

Figure 3 A measuring system for determining the value of q in one-way circulation of heat flow

Figure 4 A measuring system for determining the value of q in the two directions of circulation of heat flow

5 Conclusions

The above mentioned system can be used for:

- measuring the heat flow density in the residence (action) of person, at one point and in one direction of heat flow (e.g. xy – parallel to the floor) and comparing with requirements to ensure thermal comfort - system 1D (dimension),
- measuring the heat flow density in the residence (action) of person, at one point and in two directions (e.g. xy – parallel to the floor, xz – parallel to the outer wall 1) and comparing with requirements to ensure thermal comfort – system 2D,
- measuring the heat flow density in the residence (action) of person, at one point and in several directions (e.g. xy – parallel to the floor, xz – parallel to the outer wall, yz – parallel to the inner wall 1) and comparing with requirements to ensure thermal comfort - system 3D,
- measuring the heat flow density in the residence (action) of person, at several points simultaneously (multiple systems) and continuous recording of changes and for the subsequent creation of the map of heat flows in space. According to the choice of the system 1D and 3D, there are also given the possibilities of image,
- determining the integrated operation of heat flows from multiple sources that may be affected by a radiation component. Determination of the influence of different heat flows to devices or sensitive equipment or technology, where the stationary climatic conditions are necessary,
- verifying the program solutions (simulations of the size and direction of heat flows) with the real state.

The reference list

[1] CHUNDELA, L.: *Ergonomie, ČVUT v Praze 2007.*

[2] LORKO, M.*: Ergonómia vo výrobe, TUKE FVT, Prešov 2001.*

[3] JOKL, J., ŠENITKOVÁ, I.: *Interná mikroklíma, TU Košice , 1993.*

[4] Ahlborn Mess- und Regelungstechnik GmbH, System ALMEMO, [Online], Available: http://www.ahlborn.com/Almemo.html [24 Jun 2019]

[5] FLIMEL, M.,BALARA, M.: *Zariadenie na meranie hustoty tepelného toku v priestore, zverejnená patentová prihláška SK 50058-2015, ÚPV Banská Bystrica 2015*

Acknowledgements

The author would like to thank the KEGA grant agency for supporting research work and cofinancing the project KEGA 004TUKE-4/2018.

Advances in Thermal Processes
and Energy Transformation
Volume 2, 2019, JABL01, pp 28-33
ISSN 2585-9102

Proposal for Experimental Countercurrent Gas Generator

Gustáv Jablonský[1] ● Augustín Varga[1] ● Ladislav Lukáč[1]● Ján Kizek[1]● Marcel Pástor[1]

[1] Technical university of Košice, Faculty of Materials, Metallurgy and Recycling, Institute of Metallurgy, Letná 9, 042 00 Košice, Slovak Republic,
gustav.jablonsky@tuke.sk, augustin.varga@tuke.sk, ladislav.lukac@tuke.sk

Category : Original Scientific Paper
Received : 17 June 2019 / Revised: 27 June 2019 / Accepted: 28 June 2019

Keywords : gasifier, feeder, air supply, biomass, downdraft, specific gasification rate

Abstract : Article focuses on the description of the experimental gasification reactor design, those has been designed to solve the needs of the project VUKONZE. The characteristics of the low - power gasification generators show to problems with increased tar production, the relatively low calorific value of the gas produced as well as the supply and redistribution of the gasification air. The paper points out the differentiation of the area thermal load of the reactor in comparison with the general parameters for this kind of reactors. An integral part of the design of the reactor is also the location of the fuel charging point and the way of its realization.

Citation: Jablonský Gabriel et al.: Proposal for Experimental Countercurrent Gas Generator, Advance in Thermal Processes and Energy Transformation Volume 2, Nr.2 (2019), p. 28-33, ISSN 2585-9102

1 Introduction

The Department of Thermal Technology and Gas Industry on the Institute of Metallurgy focused on the project of VUKONZE for the constructing of a wood biomass gasification reactor with a 75 kW gas input. The produced gas is then to be used in a cogeneration unit for the production of heat and electricity. For reason necessary to verify the functionality of the design of the reactor and obtain more precise information about the relationship between the charge - gasified air and produced gas it acceded to construct experimental model with expected output of the gas 15 kW. This model device is intended to acquire large knowledge and information for the design of the above mentioned gasification reactor and the influence of various factors on the gasification process.

The design and selection of the biomass gasification generator is based on the required thermal load, charge properties, operator's demands and the possibility of modifications to the proposed reactor.

The input parameters of the generator type selection are gas output to 15 kW, charge with humidity to 30% and grain size to 20 mm. These chemical and material parameters are characteristic of the local supply of heat to the home, particularly in rural areas, and therefore the proposed model may be a model for such application.

Based on the required power, humidity, ease of service and flexibility of operation, a cohesive-layer countercurrent generator appeared to be the most suitable solution.

Of course the selection was the recognition of the disadvantages of this type of generator, as the ash removed by melting, low temperature off-gas and the consequent production of high temperature tar (well above 100 $g.m^{-3}$ [1-2]). Furthermore, an increased content of dust particles in the product gas is also provided.

2 Parameters influencing reactor design

The basis of each design is the calculation of input parameters such as the amount of charge, the choice of the most appropriate air excess and thus the amount of gasification air. Based on these parameters, we can subsequently design a gasification reactor.

The calculation for the different fuel consumption effects for the required gas performance was performed for a fuel with the following composition in running order: C = 46 wt%, H = 5.56 wt%, O = 39.5 wt%, N = 0.27 wt%, A = 0.67 wt%, W = 8 wt%.

2.1 Effect of net calorific value on reactor fuel consumption

The calorific value of the gas significantly affects the amount of charge required to achieve the desired gas output. Knowing the parameters of the charge and the type of gasification technology predetermines the delimitation of the calorific value of the gas. For gasification in the cohesive layer, the optimum gas calorific value is 4.5 - 6 MJ.m^{-3} [3]. Figure 1 shows the effect of the calorific value on the amount of fuel consumed at different outputs.

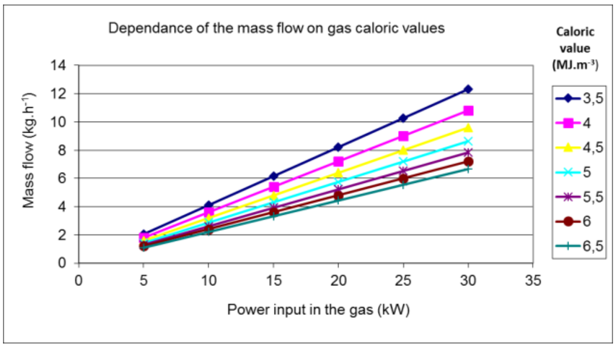

Figure 1 Dependence of the mass flow of the charge on the power input in the gas at different gas calorific values

Based on the calculations performed, the results which are shown in Figure 1 shows that a gas calorific value of 6.5 MJ.m^{-3} consumes 25% less fuel than a calorific value of 4.5 MJ.m^{-3}, assuming a gas/fuel ratio of 2 m^3.kg^{-1}. Again, such a characteristic affects the design of the gasification reactor, in particular to control the power and quantity of the gasification medium [4].

2.2 Effect of gas / fuel ratio on reactor fuel consumption

A very important parameter for the design of the reactor is the volume of gas produced per unit amount of charge (gas/fuel ratio or also V/m). This ratio is heavy expected to exhibit and as was already mentioned, this ratio will depend not only on the excess of the gasifying medium, but also the composition of the charge and temperature in the reactor.

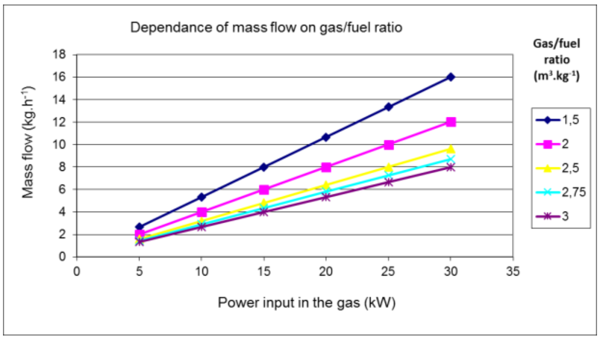

Figure 2 Dependence of mass flow rate on gas output at different gas/fuel ratio

Figure 2 shows the effect of the V/m ratio on fuel consumption for the desired power output.

The effect of the gas/fuel ratio very substantially represents the amount of fuel needed for the thermal output of the reactor. The graph dependence was processed for the gas calorific value 4.5 MJ.m^{-3}. As can be seen from the graph on Figure 2, the production of 3 m^3 of gas reduces fuel consumption by to 50%. This dependence is necessary for reactor design, but rather depends on excess air and charge parameters.

However, if we use empirically obtained stoichiometry according to which

$$1.0Biomass + 7.607Air \rightarrow 2.407CO + +2.079H_2 + 0.181CH_4 + 1.3CO_2 + 6.078N_2 + 0.158H_2O + 0.064Coke + 0.0547Tar \quad (1)$$

then the ratio of the gas produced to normal conditions to the unit amount of fuel is 2.662 Nm^3.kg^{-1}. This ratio applies to a wood chip of moisture of 10 wt%. [5]. However, such stoichiometry is specific to the fuel of the composition only.

In general, it can be assumed that not only temperature, but also residence time contributes to the amount and composition of the gas produced [4].

2.3 Gasification air excess

If the gasification process requires partial oxidation, it is necessary to know the most suitable excess of gasification medium for the quality of the produced gas. From the excess gasification air quality of the product gas is clear, by zero air excess of occurs pyrolysis. Hydrogen concentration in the emitted gas is on maximum, the gas contains almost no nitrogen, the concentration of which is derived only from the fuel. Air excess higher than one represents combustion. Growth the air excess above zero means increasing the nitrogen concentration in the gas and increasing the volume. The literature indicates that with an air excess of 0.25, all biomass is converted to gas and gas has the highest energy value [6]. A smaller air excess describes a situation in which all biomass is not converted to gas. At a higher excess occur combustion, lowering of the energy value and temperature increase. Air excess of 0.25 indicates the concentration of the combustible CO is the maximum, and CO_2 minimum. The CH_4 concentration is also minimal, but due to the increased gas volume, the calorific value of the gas is taken over by the combustible components H_2 and CO.

In some cases, the excess gasification air is calculated from the nitrogen balance based on an analysis of the gas taken at a given temperature. The gasification ratio is then the ratio of the amount of gasification air at a given temperature to the stoichiometric amount of air [7]. But what is the path leading to control and knowledge already for existing gasification reactors.

3 Design of Reactor Parameters

The design of generator parameters was based on the design of the counter-current generator, which was used in Department of Thermal Technology and Gas Industry in 2005-2010 with a gas input about 60 kW. Grain size was to 30 mm and humidity to 35%. The assumed volume of gas produced is about 2.5 times the weight of the feed with a calorific value of 4.5 MJ.m^{-3} [8].

3.1 Effect of gas / fuel ratio on reactor fuel consumption

The input data for the calculation of the reactor parameters is the reactor diameter. The calculation was based on maintaining the thermal load of the sample reactor. To calculate the reactor diameter, it is necessary to calculate:

• *amount of energogas depending of the gas type*

$$V_{EP} = \frac{Q_{EP}}{Q_{n,EP}} \tag{2}$$

V_{EP} - volumetric overflow of energogas (m^3.s^{-1}),
Q_{EP} - energogas power output (W),
$Q_{n,EP}$ - energogas calorific value (J.m^{-3}).

• *mass flow of the fuel* - the volume of the resulting biogases at a determined ratio of gas/fuel (V/m)

$$m_{PAL} = \frac{V_{EP}}{(V/m)} \tag{3}$$

m_{PAL} - fuel mass flow (kg.s^{-1}),
(V/m) - amount of energogas generated from the unit of fuel (m^3.kg^{-1}),

• *power input in fuel*

$$Q_{PAL} = m_{PAL}.Q_{n,PAL} \tag{4}$$

Q_{PAL} - fuel power input (W),
$Q_{n,PAL}$ - fuel calorific value (J.kg^{-1}),

• *thermal load*

$$q_{PAL} = \frac{Q_{PAL}}{S} \tag{5}$$

q_{PAL} - thermal load (W.m^{-2}),
S- area related to the reactor cross-section (m^2).

Considering the preservation of the thermal load of the reactor, it follows that the ratio of the cross-sectional areas will be equal to the ratio of the feed charge as well as the ratio of heat outputs. These considerations, however, are based on the assumption that heat losses are neglected.

The reactor diameter was then determined from the area to gas input ratio

$$\frac{S}{S_n} = \frac{Q_{EP}}{Q_{EP,n}} \tag{6}$$

S_n - area of the proposed reactor (m^2)
$Q_{EP,n}$ - power output in energogas of proposed reactor (W).

The input parameters for calculating the diameter of the proposed reactor are: gas power output, fuel calorific value, V/m ratio and sample reactor diameter. To calculate the diameter of the proposed reactor, it is considered that: the calorific value of the produced gas, the calorific value of the fuel and the ratio of the gas produced per unit of fuel are identical. Table 1 shows the input parameters of the exemplary reactor and the parameters of the proposed reactor.

Table 1 Comparison of parameters of sample reactor and designed reactor

Q_{EP}	60	15	kW
$Q_{n,EP}$	**4,5**		MJ.m^{-3}
V_{EP}	48	12	m^3.h^{-1}
V/m	**2**		m^3.kg^{-1}
m_{PAL}	24	6	kg.h^{-1}
$Q_{n,PAL}$	**16,84**		MJ.kg^{-1}
Q_{PAL}	112,25	28,06	kW
q_{PAL}	**802**		kW.m^{-2}
S	0,14	0,035	m^2
d	0,422	0,211	m

3.2 Height of the reactor

The upstream reactor is characterized by a long residence time. The reactor height should not be too large due to higher heat losses. However, a low reactor may not be sufficient to carry out the entire gasification process. Therefore, the height of the gasification part of the reactor is chosen mainly based on experience and estimates.

3.3 Inlet pipe diameter

The diameter of the air supply pipe does not have a significant effect on the gasification process. One possibility of designing the pipe diameter is to use the current at Department of Thermal Technology and Gas Industry reactor while maintaining the velocity profiles. Another option is related to the design of the nozzle resp. air inlet under the grate.

3.4 Gasification air preheating

An integral part of the gasification reactor design is the use of heat losses through the reactor walls. The largest part of the losses involved the vertical cylindrical part of the reactor. Location of reactor main part into a container in which is air preheated is one of effective solutions preheating the incoming air to minimize heat loss surface of the reactor.

While the reaction temperature dependence of the increase is linear, and any rise in temperature of the gasification air at 100°C will increase the temperature in the reaction part of about 40°C. The temperature increase in the reactor may also have a negative effect on the gasification, by increasing the temperature too much, especially when using fuel with a low ash melting point.

It appears that preheating of the gasification air does not have a very significant effect on the quality of the gas produced, but in particular on the reaction temperature [9-10].

3.5 Gas outlet

The term gas outlet means not only the location of the outlet pipe, but also its diameter. Gasification produces about 2.5 times the enrgogas to gasification air [8]. In this respect, it could be assumed that the outlet pipe should have a maximum cross-sectional area of 2.5 times the supply pipe. However, the temperature of the inlet air and the outlet gas must also be taken into account. The outlet pipe diameter is chosen lower to increase the reactor pressure, which has a positive effect on the quality of the gas produced in the reactor [11].

3.6 Nozzle

The introduction of the gasification medium into the oxidation zone has a considerable influence on the quality of the produced gas and the temperature distribution after the reactor cross-section. The design of the feed is based on the assumption that the gasification medium is supplied as uniformly as possible to the coke particles (charged fuel) after pyrolysis and the formation of an oxidation zone throughout the reactor cross-section. This should limit the reduced efficiency of carbon conversion. However, if we work with a substoichiometric excess of gasification medium, it is assumed that the conversion efficiency will not be unitary, thus not equal to 100%. The lower carbon conversion results in a low excess of gasification medium, loss of heat by unburnt, the possibility of non-access of oxidant to the coke particles, or the non-gassing of a part of the wood chips.

For the gasification reactor, one nozzle was selected with the gasification medium outlet at four levels. The lower 3 levels should direct the gasification medium horizontally in 6 different directions. At each level, the exit direction is rotated 30° from the previous level. High level and opening the fourth gasifying medium at an angle of approximately 55° to the upper layers of the charge, Figure 3.

However, such a nozzle may not adequately feed the gasification medium, and therefore other options must be considered and compared to the current design.

Figure 3 Cross section of proposed nozzle

3.7 Feeding proposal

For the sake of simplicity of design and the possibility of quick verification of the functionality of the device, the proposed system of feeding from ball valves is located in the upper part of the reactor. The pyramid-shaped main container is separated from the intermediate reservoir by the first ball valve and the intermediate reservoir from the gasification chamber separated by the second. This two-bolt design is selected for the following reasons:

- the need to regulate the dosage,
- ensuring the tightness of the system.

Depending on the amount of fuel supplied, the power output of the gasification generator varies, thereby regulating the amount of generated energogas. The amount of chips to be dosed is limited by the size of the intermediate tray and the number of doses per time interval.

The tightness of the system is ensured by a system of two ball valves, which by alternate opening always creates a closed space of the gas generator and thus prevents gas leakage into the surroundings of the gasifier. The problem, however, is that the solution is impractical, mainly because of the need for manual control. Frequent opening and closing of the valves is required at an average number of 2 times per minute. As with the knife closure system, there may be problems with valve closure due to chip sticking, which impairs the tightness of the device [12].

4 Design of Reactor Parameters

Based on previous dependencies, calculations and in some cases also using assumptions, the following geometrical parameters of the counter-current gasification generator of wood biomass were proposed table 2.

An experimental physical model was constructed according to the proposed geometric parameters. The gasification air enters the inlet ring to preheat the air through the supply line. After heating, it exits through a conduit for supplying preheated air to a nozzle which is connected to this conduit.

Table 2 Basic geometric parameters of the reactor

Description	Size (mm)
height of the gasification part of the reactor	**1016**
reactor inner diameter	**206**
width of annulus for preheating gasification air	**20**
inner diameter of the gasification air supply pipe	**20**
inner diameter of the gas-gas outlet pipe	**25**
ashtray height	**220**
ashtray inside diameter	**206**
nozzle diameter	**20**
nozzle height above grate	**84**
the diameter of the gasification air outlets from the nozzle	**4**
inner diameter of charging pipe	**60**
width of free cross section of grate	**7**

Preheated gasification air enters the reaction section through the nozzle and oxidizes the feed. The produced gas rises in the vertical direction, through the following zones of the gasification and exits through the outlet conduit of biogases located about 250 mm below the ceiling of the reactor. Through the charging port located in the ceiling of the reactor, continuously batches fuel - wood chips. The chips pass through the zones of drying, pyrolysis, reduction and oxidation. The remainder of the gasification - the ash falls through the grate into the ashtray, from where it is subsequently removed.

5 Conclusion

The aim of proposal experimental countercurrent gasifier generator was to design parameters of counter generator and point out the various options in design - air supply, maybe a quick adjustment of the nozzle, the location and geometry of the exhaust gas production. Based on the analysis carried out in the design of the generator shows what the experimental generators are similar and what distinguishes them. The main difference is the realization of continuous feed to the reactor, the solution of the air supply and the reactor power output.

6 The reference list

[1] YAMAZAKI, T., KOZU, H., YAMAGATA, S., MURAO, N., OHTA, S., SHIYA, S., OHBA, T. : Effect of superficial velocity on tar from downdraft gasification of biomass, *Energy Fuels*, Vol. 19, No.3, pp.1186-1191, 2005

[2] MORF, P., HASLER, P., NUSSBAUMER, T.: Mechanism and kinetics of homogeneous secondary reactions of tar from continuous pyrolysis of wood chips, *Fuel*, Vol.81, No.7, 2002, pp.843-853

[3] CHEN, C., JIN, Y., YAN, J., CHI, Y.: Simulation of municipal solid waste gasification for syngas production in fixed bed reactors, *J. Zhejiang Univ. Sci. A*, Vol.11, No.8, pp.619-628, 2010

[4] JABLONSKY, G., KIZEK, J., KOTTFEROVA, N.: *Vplyv parametrov na návrh reaktora*, Metalurgia Junior 2012, Košice, 2012, pp. 217-221, 2012

[5] RAO, M.S., SINGH, S.P., SODHA, M.S., DUBEY, A.K., SHYAM, M.: Stoichiometric, mass, energy and exergy balance analysis of countercurrent fixed – bed of post - consumers residues, *Biomass and Bioenergy*, Vol.27, No.2., pp. 155-171, 2004

[6] OCHONDEK, T. – KOLONIČNÝ, J. – BRANC, M.: *Technologie pro přípravu a energetické využití biomasy*, Ostrava, VŠB TU, 2007

[7] NAJSER, J.: Sesuvný zplyňovač s řízeným podáváním paliva, Sborník příspěvků ze semináře „Energie z biomasy X“, VUT v Brně, 2009 [Online], Available: http://biom.cz/cz/odborne-clanky/sesuvny-zplynovac-s-rizenym-podavanim-paliva [16.03.2009], 2009.

[8] HORVÁTH, L.: Analýza prúdenia v horúcom filtri čistenia plynu zo splyňovania biomasy. Dissertation thesis. TUKE, Faculty of Metallurgy, 2006. p.219

[9] BABU, B. V. –SHETH, P. N.: *Modeling and Simulation of Biomass Gasifier: Effect of Oxygen Enrichment and Steam to Air Ratio*, Proceedings of the International Congress on Renewable Energy (ICORE-2005), Birla Institute of Technology and Science, Rajasthan, India, pp.20-22, 2005

[10] JABLONSKY, G., VARGA, A., LUNKIN, V., KIZEK, J., FURKA, F.: Design of the experimental counter-current gasifier feed device, The application of experimental and numerical methods in fluid mechanics and energy 2012, Demänovská dolina, p. 87-91, 2012

[11] KUMAR, M.S., VIVEKANANDAN, S.: Effect of design and operating parameters on the gasification process of biomass in an updraft fixed

bed: a statistical study, Int. J. Chem. Sci., Vol.14, No.4, pp.2397-2419, 2016

[12] SHETH, P.N., BABU, B.V.: *Effect of Moisture Content on Composition Profiles of Producer Gas in Downdraft Biomass Gasifier*, Proceedings of International Congress Chemistry and Environment (ICCE-2005), Indore, India, pp. 356-360, 2005

Acknowledgement

This paper is the result of the Project implementation: Research centre for efficient integration of the renewable energy sources (VUKONZE), ITMS: 26220220064 supported by the Research & Development Operational Programme funded by the ERDF.

Advances in Thermal Processes and Energy Transformation
Volume 2, 2019, Pusk01, p. 34-42
ISSN 2585-9102

Analysis of Influence of the Atmospheric Conditions and Temperature Range in the Exhaust Pipe on the Output Engine Characteristics

Michal Puškár[1] ● Dušan Puškár[2]

[1]Faculty of Mechanical Engineering, Technical University of Košice, Letná 9, 04200 Košice, Slovakia, michal.puskar@tuke.sk
[2] Faculty of Mechanical Engineering, Technical University of Košice, Letná 9, 04200 Košice, Slovakia, dusan.puskar@tuke.sk

Category : Original Scientific Paper
Received : 17 June 2019 / Revised: 27 June 2019 / Accepted: 28 June 2019

Keywords : engine characteristics, atmospheric conditions, fuel efficiency

Abstract : The piston combustion engine, which is working on the HCCI technology principle, is very sensitive to changes of the external atmospheric conditions. These changes are immediately influencing the engine power characteristics. At best only they effect decreasing of the maximum engine power. However, in a more difficult situation, there is the possibility of excessive detonation combustion process during certain changes in atmospheric conditions. The exhaust system temperature significantly affects the maximum output power and the combustion engine characteristics. With increasing temperature of combustion products in the exhaust system there is an overall reduction in maximum power and its transfer to a higher engine speed because of the length of an exhaust manifold is theoretically shorten. Therefore, to achieve the maximum values of output parameters, it is necessary to ensure an optimal temperature value of the combustion products in the exhaust system. This article also provides optimal temperature range of working temperature as well as it presents a theoretical analysis of the impact for atmospheric conditions in this interval. Based on theoretical results there has been developed a measuring method, which allows to regulate the input amount of the fuel mixture supplied to a cylinder during change in atmospheric conditions and its functionality was experimentally verified.

Citation: Puškár Michal, Puškár Dušan: Analysis of Influence of the Atmospheric Conditions and Temperature Range in the Exhaust Pipe on the Output Engine Characteristics, Advance in Thermal Processes and Energy Transformation, Volume 2, No.2 (2019), p. 34-42, ISSN 2585-9102

1 Introduction

An exhaust system is the important supplement of the all engines. It has got the determining influence on engine outgoing parameters for the engines with two-stroke operating cycle. Gas flow in an exhaust system is controlled by means of the difficult principles of non-stationary convection with very difficult calculation. Although the existing special software reached the certain voluminous results, the main merits of work are still in the verification of calculated values on a testing engine [1]. In practice, in most motorcycle firms, which are the leaders for development, there are designed several modifications of exhaust systems according to generally known rules. These modified systems are tested and consequently improved with output brake engine tests. One exhaust system is suitable theoretically only for one value of engine speed. It is rather small speed range in practice. The final modification of exhaust system is accommodated to the most using speed values considering the operation possibility in its other modes.

In a cylinder on a piston top edge there is an impulse created by means of the opening of exhaust port. It causes an overpressure wave, which is spreading into an exhaust manifold in existing environment with sound speed. In an exhaust manifold there is the sound speed much higher than in the open air. Exhaust manifold gases are step by step exposed the pressure wave influence. In consequence of this fact the gases begin to move outwards from an engine. But there is a reflection back of pressure wave from the opposite cone what causes the gas oscillation following a longitudinal axle of an exhaust stroke. The aim of the correct dimensioned exhaust system is to improve exhaust of gases from a cylinder and this way to improve the scavenging process [4]. During scavenging of working space with overflowing streams there is the certain mixing of combustion products and fresh fuel-air mixture. The part of fresh fuel-air mixture leaks out into an exhaust port. A fuel-air mixture and combustion products mixing continues there. Close by an engine the gas mixture contains rather few combustion products. That is why there is the effort dimensionally to dispose the exhaust system so that the back movement occurs in the final phase. This back movement comes into existence by reason of the oscillation and again there is the return of off-take gases into the cylinder working space. The fuel-air mixture, which contains lower percentage of combustion products, can be used at combustion [2].

The aim of this contribution is to develop a measurement method solving the problems of output characteristics for high-speed racing engines caused by change in atmospheric conditions based on theory of optimal temperature range of the exhaust system.

The following steps are connected to this main aim:

- analysis of combustion product temperature influence in an exhaust system on a maximum engine output and its position in engine speed range
- estimation of an optimal temperature range
- theoretically definition of the influence of atmospheric conditions on mixture composition and so the exhaust system temperature will effect and subsequent development of software
- performance of measurements to verify the theoretical data and developed software.

2 Experimental Models and Measuring Devices

It is difficult to work theoretically on the development of individual components and then to demonstrate their influence on the parameters of petrol engine power and torque. Although there is the software for a modelling of processes, which are operating inside a cylinder and an exhaust system during combustion, the real results are performed seriously. That is why the experiment was used to achieve the main aim. It is necessary to choose the experimental model for experimental measurements. The development was realised with this experimental model. Further it is a need to choose the measurement device (to provide feed back, to give information about a real output proposition for concrete change).

2.1 Experimental Model

The petrol combustion engine with capacity 125 cm^3 was used as the experimental model. The specifications of the engine used in the test are shown in Table 1.

Table 1 Technical Parameters of Test Engine

Type	a single-cylinder engine, liquid cooled, membrane filled, an electrical-controlled exhaust power valve
Capacity	124.8 cm^3
Bore x Stroke	54 x 54.5 mm
Type of exhaust	resonance exhaust system

As results of long-time experiences and motorcycle firms' research the resonance exhaust system is the most suitable. This shape, with small differences, is used for the large spectrum of motorcycles series as well as special racing vehicles [6].

An ignition curve, its shape is given with a graphic representation by means of the pre-ignition degrees in dependence on an engine speed, was developed considerably. The newest and the latest shapes of ignition curves are common curves, which eliminate the inadequacies, for example the problems with a filling for the concrete mode of an engine speed [5]. For the needs of the experimental measurements there was used standard ignition curve of tested engine.

Unleaded petrol with the octane number 100 was applied as a fuel.

2.2 Measuring Device

For a need of the experimental measurements were developed testing and measuring device Engine Watch and Control System (EW&C).

That is a data-recording system, i.e. a device, which scans and stores information during a motorcycle ride (in real conditions, in real loading) [7]. This device makes possible to diagnose parameters of a combustion engine: an output performance, a torque and their behaviours, a temperature of exhaust system and its behaviour and other characteristics. A number and a kind of scanned parameters are related to the types and a number of sensors, which are installed on the combustion engine.

In Figure 1 there is the block diagram for data measurement, operating and evaluation. The engine activity record in dependence on time is the result of this system. The principle of EW&C system consists in the measurement of instantaneous engine revolutions; an instantaneous temperature of exhaust system and a reading of an active speed gear or throttle position in carburator.

The system does a functional record of engine activity on the basis of scanned and entered data (a wheel circumference, gear ratios of individual speed gears, a curve of air resistance and a motorcycle weight). This record is stored in the memory of EW&C system. After finishing of the measurement, it is possible to copy the record into PC.
On PC display (Figures 2, 3, 4, 6, 7) there is the record of engine activity in dependence on a time axis graphically presented (by means of the software which is a component of EW&C system). Every point of the record covers an instantaneous speed, a temperature of exhaust system and an output at a crankshaft end.

3 Experimental Measurements

In the experimental model there were applied the diagnostic device, described in above-mentioned paragraph. The measurements were performed for racing circuit. The obtained results, which are presented in this paragraph, were verified with multiple consecutive measurements to prevent a potential random error.

The experimental measurements will be focused on the following areas:

The first is analysis of the combustion product temperature influence in an exhaust system on a maximum engine output and its position in the engine speed range.

The next step will be to estimate an optimal temperature range, which is necessary for the optimum engine output characteristics.

Atmospheric conditions have got the most significant influence on the optimal working temperature interval in the exhaust system. An impact of atmospheric conditions on the mixture composition will be theoretically defined and on the base of theoretical conclusions there will be developed the software. By means of this software the mixture composition will be changed, thereby providing an exhaust system optimal temperature for any conditions.

The last step will be the measurements intended to verify the theoretical bases and developed software.

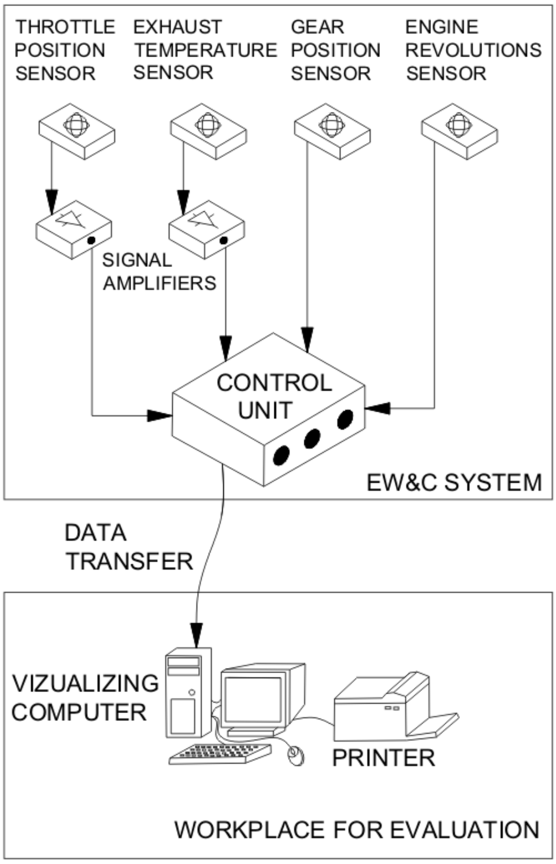

Figure 1 Block Diagram of EW&C System

3.1 Analysis of Combustion Products Temperature Influence in Exhaust System for Output Characteristic

When the exhaust system length is shortened the maximum output and the maximum torque are moved into higher operating speed of the combustion engine. That is valid at a constant temperature and a constant pressure. And similarly the sonic wave rate of spread depends on a pressure and a temperature. A sonic wave rate of spread increases with an accumulative temperature in the exhaust system. A maximum and minimum temperature exists theoretically for every exhaust system, defined shape and dimensions. The output and torque behaviours increase the most effectively in this thermal interval because the scavenging of engine cylinder is optimized by means of the exhaust system. With regard to above-mentioned assumption, the experimental measurements were performed on the base of this prediction and these measurements were intent on the explanation of combustion products temperature in an exhaust system for an output characteristic of combustion engine.

The aim of measurements was defined for the optimal operating thermal interval to achieve a maximum output for used exhaust system.

Three thermal states were used for the measurement in the exhaust system:

1. Thermal interval from 440°C to 540°C (Fig.2)
2. Thermal interval from 520°C to 620°C (Fig.3)
3. Thermal interval from 600°C to 720°C (Fig.4)

The temperature values were measured at points where the temperature of exhaust system reaches the maximum, i.e. in the area of exhaust pipe, approximately 150 mm from the upper edge of exhaust port.

In Figure 2 there is illustrated the record of engine activity and the behaviour of engine performance in dependence on a time axis. A time axis is represented in the bottom part of the figure (left part). The engine activity record is represented with an upper curve (saw-tooth type in left part).

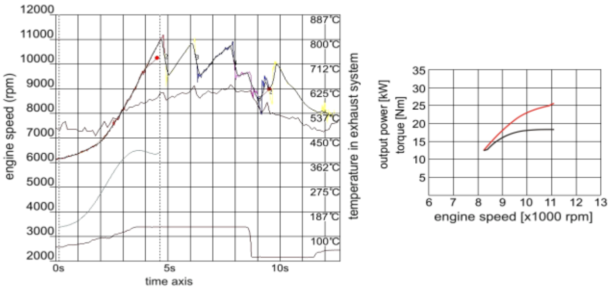

Figure 2 Activity Record and Output Behaviour of Engine in 1st Thermal State

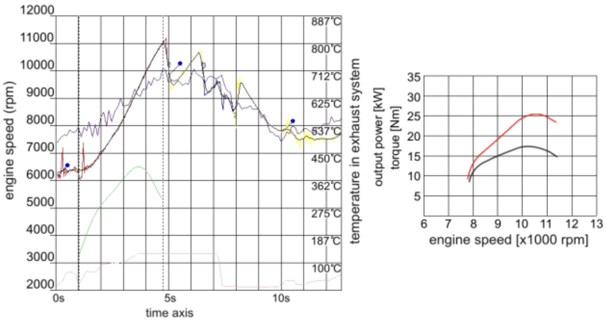

Figure 3 Activity Record and Output Behaviour of Engine in 2nd Thermal State

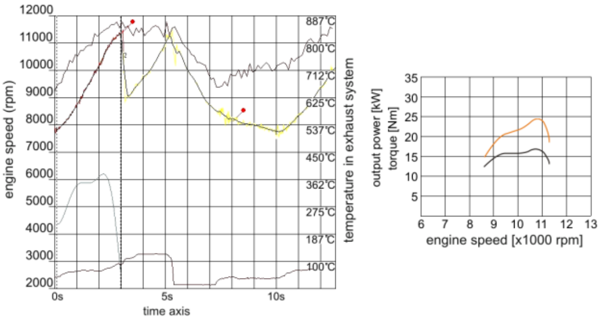

Figure 4 Activity Record and Output Behaviour of Engine in 3rd Thermal State

On the left side left part of figure there is an axis, which represents engine speed (revolutions); therefore it is possible to define the range of operating speed, which the engine operates in. The axis of temperature in the exhaust system is on the right side of left part of figure. The temperature behaviour is represented a curve given in the lower section of the left part of figure. In this case the illustrated curve is almost a line because a relevant sensor was inactive.

The concrete extent of activity engine record was selected. This extent was terminated on both sides (with dash vertical lines of left part), then was analysed with regard to an output performance. This analyse is illustrated by the graph on right side of this picture. The horizontal axis belongs to the engine speed (revolutions) and the vertical axis is for the output performance. There is an upper curve, which represents the output performance behaviour in dependence on an engine speed axis and the bottom curve belongs to the torque behaviour.

A sonic waves rate of spread increases with accumulative temperature. In the exhaust system a back wave returns quicker and so the back scavenging process of a cylinder is accelerated. Theoretically, an exhaust system is shortened.

An exhaust system temperature hast to rise with the increasing revolutions of optimal adjusted engine therefore the exhaust system is theoretically shorter at higher speed and theoretically longer (with lower temperature) at lower engine speed.

The maximum output and the range of exploitable speed, i.e. revolutions with high value of instantaneous output is constantly kept, are important parameters for the practical use.

In Tab.2 there are the measurement results, the maximum outputs and the ranges of exploitable speed in the individual thermal intervals.

Table 2 Measurement Results

	Maximum Output /Engine Speed [kW/rpm]	Range of Speed for Output over 20kW [rpm]	Maximum Torque/Engine Speed [N.m/rpm]	Range of Speed for Torque over 15 N.m [rpm]
1. Thermal interval: from 440 to 540°C	25,5 / 11,100	1,700	18 / 11,100	2,300
2. Thermal interval: from 520 to 620°C	25.6 / 10,500	2,300	18 / 10,300	2,400
3. Thermal interval: from 600 to 720°C	24.0 / 10,800	1,800	17 / 10,600	2,000

According to the measurement results analysis the shortening of exhaust system length in the area of exhaust pipe induces the transfer of a maximum output and a maximum torque to the higher operating speed of combustion engine [9]. Simultaneously the range of operating speed is wider. The next contribution is the more fluent increasing of an output and a torque what provides better steering control. This knowledge makes possible the variability of output curve according to the concrete necessity of given single-track vehicle.

According to the measurement results analysis the thermal interval from 520 to 620°C is the optimal interval of operating temperatures in an exhaust system for this combustion engine. However, the conditions are not so optimal in this interval of limited values 520°C and 620°C. The highest output is reached if the temperature converges in an exhaust system to the mean value of interval, i.e. 570°C. The temperature in an exhaust system increased with an output what is characteristic for an optimal adjustment.

In thermal interval from 440°C to 540°C there was the maximum engine output lower and the range of exploitable speed decreased as well. The exhaust system was overcooled thus theoretically shorter. That is valid predominately for the temperature 440°C. The exhaust manifold is theoretically shortened toward an upper limit of interval and the engine characteristics are improved significantly.

In thermal interval from 600 to 720°C there was the maximum engine output the lowest and there was the range of exploitable speed practically unavailable. That is valid predominately for the temperature 720°C. In lower limit of interval 600°C there are good output characteristics. The output parameters make significantly worse with the increasing temperature. The system is overheated and theoretically the exhaust manifold is excessively shortened.

In the exhaust manifold the low temperature means that there is an overrich mixture (fuel redundancy) and it follows an imperfect burning.

In the exhaust manifold the high temperature means that there is a weak mixture, it smoulders out in the exhaust manifold, the combustion process takes longer time (fuel lack).

In the exhaust manifold the optimal temperature means that the composition of mixture is optimal and heat is changed into mechanical energy with the high efficiency.

It follows that a temperature in an exhaust system has got a cardinal influence on an engine output characteristic. That is why it is necessary to ensure its optimal interval. It will be important for this thermal interval where the temperature increases proportionately with an operating engine speed and an engine load. It causes theoretically the lengthening (for lower operating engine speed) and theoretically the shortening (for higher operating engine speed) of an exhaust system. This effect provides a higher output in the whole regime of revolutions and decreases a production of emission because there is more perfect combustion here. Now, the highest efficiency of combustion engine will be provided.

3.2 Theoretical Definition of Atmospheric Condition Influence on the Mixture Composition and Development of Software

Atmospheric conditions are one of the greatest influences on a quality of mixture combustion in engine and so they affect its temperature of exhaust system [10].

In the theoretical analysis of influence of atmospheric conditions for the combustion engine parameters we considered the wet air characteristics. A wet air is the mixture of a dry air and a vapour. The gases, contained in an air, are in an overheated state and in relatively small molecule concentration that is why a dry air is instructed by almost perfect state equation for ideal gas (1). It is also possible to use the state equation for a vapour concerning its small concentration in air (1).

$$p \cdot V = n \cdot R \cdot T \qquad (1)$$

where: p – partial pressure [N.m^{-2}]

V – volume [m^3]

n – amount of substance [mol]

R – universal gas constant [J.mol^{-1}.K^{-1}]

T – temperature [K]

Total pressure of air p is equal to the sum of the particular partial pressures (Dalton's law).

$$p = p_v + p_p \qquad (2)$$

where: p_p – partial pressure of air

p_v – partial pressure of water vapour

The relative humidity φ gives the amount of water vapour which air is saturated

$$\varphi = \frac{p_p}{p_p''} \qquad (3)$$

where: p_p'' – a pressure of saturated water vapour at air temperature [3]

We formulate a partial pressure of air p_p from the expression of relative humidity or air (3) and then we institute it to the equation (2). After a substitution we can formulate a vapour partial pressure p_v from Dalton's law.

$$p_v = p - \varphi \cdot p''_{p(T)} \qquad (4)$$

From the state equation (1) we can formulate the amounts of substance for an initial and a final changed state of atmospheric conditions. We assume a constant volume.

$$n_{v1} = \frac{p_{v1} \cdot V}{R.T_1} \qquad (5)$$

$$n_{v1} = \frac{p_{v1} \cdot V}{R.T_1} \qquad (6)$$

By comparing the relations (5) and (6) we get the relation for a ratio of dry air molar amounts.

$$\frac{n_{v2}}{n_{v1}} = \frac{p_{v2} \cdot T_1}{p_{v1} \cdot T_2} \qquad (7)$$

If : $\frac{n_{v2}}{n_{v1}} > 1$

then ignition mixture was depleted with an influence of change of atmospheric conditions. It is necessary to increase a needed amount of delivered mixture regarding a maximum output regain.

If : $\frac{n_{v2}}{n_{v1}} < 1$

then by influence of atmospheric condition changes there was an enrichment of combustion mixture. It is necessary to decrease an amount of supplied mixture regarding an achievement of maximum output.

They are several possibilities to correct the supplied amount of combustion mixture. For the engines with carburators there are the changes of a carburator set-up (flow intensity of the main jet, stroke height of a jet needle, type and size of a needle jet holder or shape and size of a throttle valve). For the engines with fuel injection there is a possibility to reprogram a fuel map.

On the base of theoretical analysis according relations (4) and (7) there was a program assembled, called the Mixture Calculator. It enables a practical and a quick calculating of a necessary change in a mixture richness setup according to a change of atmospheric exposure. The data of two states are the input ones of this program. The fist state is characterised with the initial parameters (temperature, pressure, humidity) during which a maximum output was reached. The second state is characterised by the actual parameters (temperature, pressure, humidity) of a barometer reading ambient air. The software output is a correction of a mixture amount expressed as a percentage.

The aim of measurements was to test the functionality and accuracy of the assembled program Mixture Calculator and the operative influence of atmospheric conditions on an output characteristic of the combustion engine and temperature of exhaust system.

The measurements were performed in the racing circuit and measurement No.1 and No.2 were performed during different atmospheric conditions. Then, by means of the developed software there was done the regulation of fuel map.

In Table 3 there are scheduled the atmospheric conditions for each of measurements. In Table 4 there are recorded numerically the fuel maps which then in Figure 5 there are illustrated.

Table 3 Atmospheric Conditions

No.	Atmospheric Conditions		
	Temperature [°C]	**Pressure [Pa]**	**Humidity [%]**
1	20.5	96.4×10^3	68
2	24.7	96.9×10^3	49

Table 4 Fuel Maps

No.	Throttle Position [%]								
	0÷20	30	40	50	60	70	80	90	100
1	90	98	128	157	185	212	239	264	288
2	90	90	118	148	176	204	230	256	280

Table 4 contains the fuel maps. In upper row there is given the percentage positions of throttle. In left column there is the consecutive number of measurement, so every row represents one map.

The numerical value, given for concrete position of the throttle, represents a flow space. Through this flow space there is a fuel flowed into a diffuser of carburator. Subsequently in the diffuser there is an influent fuel mixed with air. These values help to do comparison of various alternatives for fuel maps. If a value is higher then represents over-richer alternative for the concrete carburator set-up and on the other hand if a value is lower then there is the mixture weakened.

The fuel map of measurement No. 2 was depleted on the base of change of atmospheric conditions and results from the program Mixture calculator. It means that the flow space, through which fuel flows in the carburator for a mixture development, was reduced.

In Figure 5 there are illustrated the fuel maps. The wetted cross-section is a dimensionless parameter and represents a value of flow space, which flows a fuel through, referred in the special unit, [$mm^2 \cdot 100$]. This diagram was drawn on the basis of numerical data from Table 4. This graph makes possible to obtain more integrated view of the fuel supplies at all kinds of measurements. A horizontal axis represents the throttle position and a vertical axis is given for the wetted cross-section. Fuel flows through this flow space in the carburator at a determined time. Its value is referred in absolute numbers.

In Fig.6 and Fig.7 there are illustrated the records of engine activities (left) and the output behaviours (right) under both atmospheric states. They are the records of engine activity in dependence on a time. A time axis is represented in the bottom part of the figure. The engine activity record is represented with an upper curve (saw-tooth type). On the left side there is an axis, which represents an engine speed; therefore it is possible to define the range of engine operating speed.

The axis of temperature in the exhaust system is on the right side. The temperature behaviour is represented by a curve given in the lower section of the figure. In this case the illustrated curve is almost a line because a relevant sensor was inactive.

The concrete section of the activity engine record was selected. This section was terminated on both sides (with dash vertical lines), then was analysed with regard to an engine output. This analyse is illustrated in the right graph. The horizontal axis belongs to the engine speed and the vertical axis is determined for the actuator output. In this graph there is a curve, which represents the output behaviour in dependence on an engine speed.

Three equal stages in three measured laps of the racing circuit were selected for the analysis of an output because a selection of only one measured stage and one curve could be responsive to an occurrence of a random error.

The deviations within the group of output curves are caused by the external influences e.g. a different exit speed from the turn to the finish line where the output analysis was done.

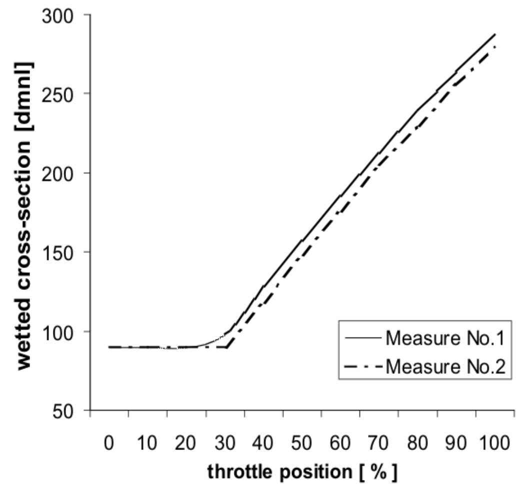

Figure 5 Fuel Maps

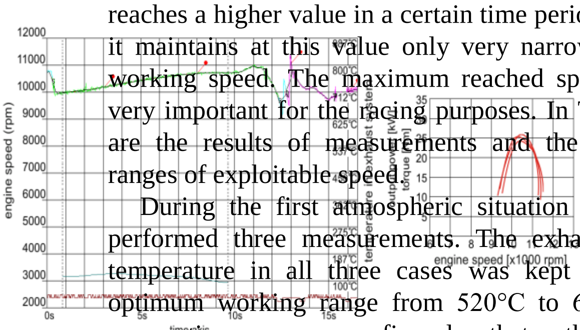

Figure 6 Activity Record (left) and Behaviour of Engine Output (right) in 1st Atmospheric State

Table 5 Measurement Results

In term of view of a practical application the most important parameter is the range of exploitable speed of an engine. At this speed there is the constantly high value of an instantaneous output maintained. It is irrelevant for an optimal engine setup if the output reaches a higher value in a certain time period however it maintains at this value only very narrow range of working speed. The maximum reached speed is also very important for the racing purposes. In Tab.5 there are the results of measurements and the individual ranges of exploitable speed.

During the first atmospheric situation there were performed three measurements. The exhaust system temperature in all three cases was kept within the optimum working range from 520°C to 620°C. Our assumption was confirmed that the output characteristics are the best when the temperature converges to the mean value of 570°C. During the second atmospheric situation there were realized also three measurements. The results were comparable to the results from the first situation and again the highest performance was at the mean temperature in the exhaust system.

It is important finding that in both situations on the basis of this method there was possible to keep an optimal temperature range of the exhaust system, although the atmospheric conditions have been changed.

	No. Curve	Temperature of Exhaust system [°C]	Maximum Output /Engine Speed [kW/rpm]	Range of Speed for Output over 20kW [rpm]	Maximum Torque/Engine Speed [N.m/rpm]	Range of Speed for Torque over 15 N.m [rpm]
1st Atmospheric State	1	571	26.0 / 10,500	1,500	18.0 / 10,300	1,600
	2	532	25.5 / 10,300	1,500	17.2 / 10,200	1,500
	3	615	24.2 / 10,300	1,300	17.0/ 10,300	1,400
2st Atmospheric State	1	573	26.0 / 10,450	1,500	18.0/ 10,300	1,600
	2	539	25.5 / 10,400	1,500	17.2 / 10,200	1,500
	3	622	24.5 / 10,500	1,300	17.2 / 10,300	1,400

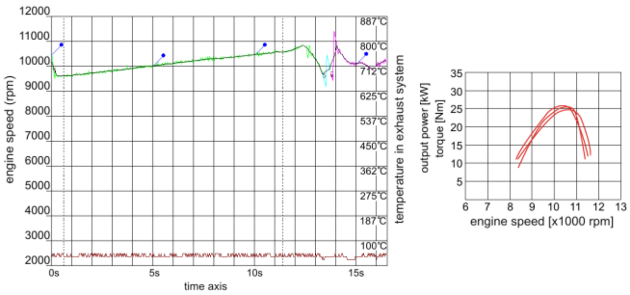

Figure 7 Activity Record (left) and Behaviour of Engine Output (right) in 2st Atmospheric State

4 Conclusions

On the base of measurement results analysis it is possible to state that the applied theoretical conclusions as well as the assembled program are exact and by means of this software it is possible with good accuracy to optimally set up the filling of combustion engine. The outputs and the range of exploitable speeds are approximately equal at both compared states. The maximum reached speeds are also comparative.

This knowledge has got the great value for the top racing engines. However they are also important for common use of combustion units in single-track vehicles. According to the optimal setup of engine it is possible to reach a good output and allowable amounts of emissions, which are accentuated on the present.

This knowledge has also its significant economic relevance. From the entrepreneurial point of view, the efficiency of the engine is enhanced. As the risk of malfunctioning is mitigated, so are the costs of damages and replacements cut, and the parts of piston, as well as the head of the cylinder and the crankshafts last longer. The precursory calculations indicate that by racing engines, the total costs of producing maximal output are reduced by up to fifty percent. The reduced costs deliver competitive advantage for an entrepreneur and crucial advantage for a rider. From the broader economic perspective, also the productivity of labour is enhanced.

5 The reference list

[1] KUMAR, R.; HAN, X.; ZHENG, M.: Precise instrumentation of a diesel single-cylinder research engine, Measurement 2011; 7: 1261-1278.

[2] BIGOŠ, P.; PUŠKÁR, M.: Influence of Cylinder Shape and Combustion Space on Engine Output Characteristic of Two-stroke Combustion Engine, Zdvihací zařízení v teorii a praxi, 3 /2008, ISSN 1802-2812.

[3] BIGOŠ, P.; PUŠKÁR. M.: Vplyv atmosferických podmienok na výkonovú charakteristiku dvojtaktného spaľovacieho motora, Zdvihací zařízení v teorii a praxi, 1/2007, ISSN 1802-2812 (“Influence of Atmospheric Conditions on Output Performance Characteristic for Two-Stroke Combustion Engine”).

[4] DOGRA, S.; YADAV, S.; BANDYOPADHYAY A.K.: Computer simulation of a 1.0 GPa piston-cylinder assembly using finite element analysis (FEA), Measurement 2010, 43 (10): 1345-1354.

[5] HOU, J.; QIAO, X.; WANG, Z.; LIU, W.; HUANG Z.: Characterization of knocking combustion in HCCI DME engine using wavelet packet transform. Appl Energy 2010, 87: 1239–1246.

[6] IKRINSKÝ, A.; PATEK, P.; TICHÝ, J.: Teória dopravných prostriedkov, SjF STU Bratislava, 2007 (“Theory of Vehicles”).

[7] JUANG L.-H.: Finite element modelling for a piezoelectric ultrasonic system, Measurement 2010, 43 (10): 1387-1397.

[8] PUŠKÁR, M.; BIGOŠ, P.: Output Performance Increase of Two-stroke Combustion Engine with Detonation Combustion Optimization, Strojarstvo 2010: Vol. 52, no. 5 (2010), p. 577-587, ISSN 0562-1887

[9] PUŠKÁR, M.; BIGOŠ, P.: Method for accurate measurements of detonations in motorbike high speed racing engine, Measurement 2012, Vol. 45, no. 3 (2012), p. 529–534, ISSN 0263-2241

[10] PUŠKÁR, M.; BIGOŠ, P.; PUŠKÁROVÁ, P.: Accurate measurements of output characteristics and detonations of motorbike high-speed racing engine and their optimization at actual atmospheric conditions and combusted mixture composition, Measurement 2012, Vol. 45, no. 5 (2012), p. 1067–1076, ISSN 0263-2241

Acknowledgments

This work was supported by the Slovak Research and Development Agency under the contract No. APVV-16-0259.

The article was written in the framework of Grant Projects: APVV-16-0259 “Research and development of combustion technology based on controlled homogenous charge compression ignition in order to reduce nitrogen oxide emissions of motor vehicles”, VEGA 1/0473/17 “Research and development of technology for homogeneous charge self-ignition using compression in order to increase engine efficiency and to reduce vehicle emissions” and KEGA 041TUKE-4/2017 “Implementation of new technologies specified for solution of questions concerning emissions of vehicles and transformation of them into the educational process in order to improve quality of education.”